Science of the Total Environment 628–629 (2018) 772–781

Contents lists available at ScienceDirect

Science of the Total Environment

journal homepage: www.elsevier.com/locate/scitotenv

Morphologies and elemental compositions of local biomass burning particles at urban and glacier sites in southeastern Tibetan Plateau: Results from an expedition in 2010

Tafeng Hu [a], Junji Cao [a,*], Chongshu Zhu [a], Zhuzi Zhao [a], Suixin Liu [a], Daizhou Zhang [b,*]

[a] Key Laboratory of Aerosol Chemistry & Physics, SKLLQG, Institute of Earth Environment, Chinese Academy of Sciences, Xi'an 710061, China
[b] Faculty of Environmental and Symbiotic Sciences, Prefectural University of Kumamoto, Kumamoto 862-8502, Japan

HIGHLIGHTS

- Aerosol particles at urban and glacier sites in southeastern Tibet were analysed.
- Soot aggregates at the glacier site were from biomass burning in the plateau.
- Physically or chemically processed ageing of the aggregates were rarely confirmed.
- Locally-emitted soot may affect glaciers differently than those from South Asia.

GRAPHICAL ABSTRACT

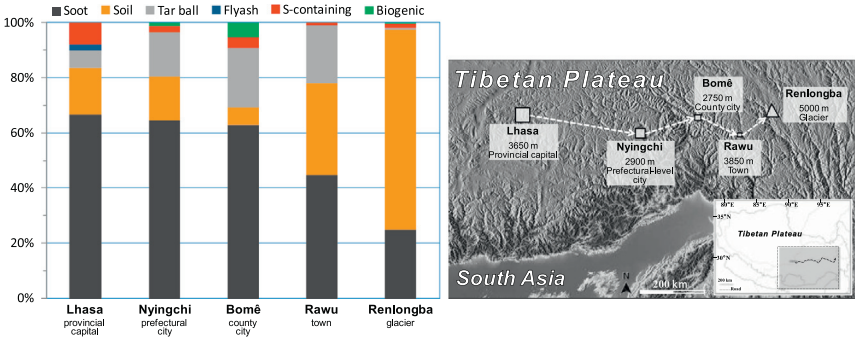

ARTICLE INFO

Article history:
Received 26 December 2017
Received in revised form 7 February 2018
Accepted 7 February 2018
Available online xxxx

Editor: Jianmin Chen

Keywords:
Tibetan Plateau
Soot particles
Ageing
Glacier area
Individual particle analysis

ABSTRACT

Many studies indicate that the atmospheric environment over the southern part of the Tibetan Plateau is influenced by aged biomass burning particles that are transported over long distances from South Asia. However, our knowledge of the particles emitted locally (within the plateau region) is poor. We collected aerosol particles at four urban sites and one remote glacier site during a scientific expedition to the southeastern Tibetan Plateau in spring 2010. Weather and backward trajectory analyses indicated that the particles we collected were more likely dominated by particles emitted within the plateau. The particles were examined using an electron microscope and identified according to their sizes, shapes and elemental compositions. At three urban sites where the anthropogenic particles were produced mainly by the burning of firewood, soot aggregates were in the majority and made up >40% of the particles by number. At Lhasa, the largest city on the Tibetan Plateau, tar balls and mineral particles were also frequently observed because of the use of coal and natural gas, in addition to biofuel. In contrast, at the glacier site, large numbers of chain-like soot aggregates (~25% by number) were noted. The morphologies of these aggregates were similar to those of freshly emitted ones at the urban sites; moreover, physically or chemically processed ageing was rarely confirmed. These limited observations suggest that the biomass burning particles age slowly in the cold, dry plateau air. Anthropogenic particles emitted locally within the elevated plateau region may thus affect the environment within glaciated areas in Tibet differently than anthropogenic particles transported from South Asia.

* Corresponding authors.
E-mail addresses: cao@loess.llqg.ac.cn (J. Cao), dzzhang@pu-kumamoto.ac.jp (D. Zhang).

https://doi.org/10.1016/j.scitotenv.2018.02.073
0048-9697/

1. Introduction

Atmospheric aerosols derived from natural and anthropogenic emission sources exert an important influence on regional and global climate change both directly, via the scattering and absorption of atmospheric radiation, and through acting as condensation nuclei in the formation of cloud droplets (Buseck and Pósfai, 1999; Kaufman et al., 2002; Akimoto, 2003). In remote glacier areas, the deposition of light-absorbing aerosol components on snow and ice reduces the albedo of these bright surfaces because the dark aerosols enhance the absorption of solar radiation; thus, this deposition accelerates the melting of glaciers and sea ice (Hansen and Nazarenko, 2004; Ramanathan and Feng, 2009; B. Xu et al., 2009; Kopacz et al., 2011; Y. Li et al., 2016; X. Li et al., 2017).

The Himalayas and the Tibetan Plateau are often referred as Earth's "Third Pole" because they contain the world's largest volume of persistent ice outside the Arctic and Antarctica. This area is also called the "Water Tower of Asia" because it contains the headwater areas of several of the major rivers of Asia. The Tibetan Plateau is a high-elevation region in Central Asia. Its average elevation exceeds 4000 m a.s.l., and its area exceeds 2.5 million km^2. Because of the low density of the air and the strong surface heating within this region, dry thermal updrafts trigger deep convection over the plateau and drive the Asian monsoon system; these processes lead to the large-scale convergence of air masses from the surrounding areas, including South Asia (Yanai et al., 1992; Liu and Yin, 2002; Lau et al., 2006). Recent observations and model studies suggest that this region is a key element of the energy cycle that makes up part of the Earth's climate system, owing to the role of this area in the large-scale circulation patterns that connect the Indian Ocean, the Asian continent and the northwestern Pacific (Zhang et al., 2001; Lau et al., 2006; B.Q. Xu et al., 2009; Kang et al., 2010; Lau et al., 2010).

Substantial evidence that the Himalayas and the Tibetan Plateau are constantly exposed to polluted air masses sourced from regions outside of the plateau, including South Asia, central Asia and East Asia, has been provided by studies based on chemical characterizations, satellite observations and numerical simulations (Loewen et al., 2007; Cao et al., 2010; Kopacz et al., 2011; Xia et al., 2011; Lu et al., 2012; S. Zhao et al., 2013; Z. Zhao et al., 2013; Cong et al., 2015; Kang et al., 2016; Lüthi et al., 2015; Fan et al., 2016; Zhu et al., 2016, 2017). Bulk analyses of chemical components (carbonaceous species, water-soluble inorganic ions, and major elements), including in situ measurements of black carbon, and filter-based measurements of elemental carbon and soot have also been carried out on the particulate matter in the plateau air (Cao et al., 2010; Engling et al., 2011; Zhang et al., 2012; Z. Zhao et al., 2013). These studies indicate that air pollutants from Bangladesh and eastern and northeastern India may travel along Himalayan valleys under certain meteorological conditions, thus reaching the southeastern part of the Tibetan Plateau; this movement of polluted air masses is called the "direct channel" (Bonasoni et al., 2010) or "leaking wall" (Cao et al., 2010) behaviour. However, a few recent studies, which have been conducted mainly in the central portion of the Tibetan Plateau and along the western Himalayas, have noted the possible significance of aerosol sources on the plateau (Li et al., 2008; Chen et al., 2015; C. Li et al., 2016; H. Li et al., 2017; Zhang et al., 2017). Unfortunately, very limited data are available on the physical and chemical properties of aerosol particles generated locally or regionally on the plateau. This lack of data is especially pronounced in the regions north of the eastern Himalayas, i.e., the southeastern part of the Tibetan Plateau, and it hinders additional and more detailed studies on the influence of locally emitted anthropogenic particles on the atmospheric and cryospheric environment.

For this study, aerosol particles were collected at four urban sites and one remote glacier site in the southeastern Tibetan Plateau during a scientific expedition. The morphologies of individual particles and their size distributions were determined using a scanning electron microscope. The elements contained in the particles were identified with an energy dispersive X-ray spectrometer attached to the electron microscope (SEM/EDX). Here, the origin and the ageing of the particles are discussed, focusing on the particles at the glacier site.

2. Methodology

2.1. Sample collection

The sample collection was carried out during a scientific expedition that extended from 12 to 18 April 2010 and was conducted along the G318 highway, the longest national highway in China, which passes through the southeastern portion of the Tibetan Plateau. The sampling sites included four urban sites at Lhasa, Nyingchi, Bomê and Rawu, and one glacier site at the remote Renlongba Glacier (Fig. 1).

Lhasa, the administrative capital of the Tibet Autonomous Region, is the biggest city on the plateau, and it has an urban population of approximately 200,000. Lhasa lies in the centre of the plateau, and its elevation is 3650 m. The highest mountain in the area surrounding Lhasa has an elevation of approximately 5500 m a.s.l. Sources of air pollutants in Lhasa include limited industrial facilities; the consumption of biofuel (dried yak dung) for household energy; the burning of coal, natural gas, and liquefied petroleum gas; and the burning of incense for religious activities. Nyingchi, which is also known as Linzhi, is a prefecture-level city located in the southeastern portion of the plateau. Its urban population is approximately 35,000. The city is surrounded by large forests, and the major energy source is firewood. Bomê, also known as Bome, is an agricultural county in Nyingchi Prefecture. Its urban population is approximately 8900 and it is surrounded by forests and mountains. Rawu, also known as Ranwu, is a small town in Baxoi county with a population of <2900. Similar to Nyingchi, the primary energy source in Bomê and Rawu is firewood. Renlongba Glacier is located in an uninhabited area approximately 60 km east of Rawu and 50 km from the G318 highway. The weather during the expedition was fine, and sunny conditions occurred on all of the days on which samples were collected.

The Tibet Autonomous Region contains 5 prefecture-level cities, including Lhasa and Nyingchi; 73 county-level cities, including Bomê; and 694 township-level towns, including Rawu (Yearbook, 2016). Domestic biomass burning is the primary source of energy in the region as a whole, and it accounted for nearly 70% of the energy produced in this region in 2003. Animal waste, firewood, and straw made up 53%, 37%, and 10% of the biomass burned, respectively (Yang et al., 2008; Wang, 2009). With respect to the potential availability of energy, forestry residues are abundant in Tibet, but agricultural residues are rare (Liu and Shen, 2007; Gao et al., 2016). >90% of the forests in Tibet are widely distributed on the southeastern Tibetan Plateau and the northern slope of the Himalayas (Peng et al., 2012; Zhang et al., 2013). Firewood serves nearly all heating and cooking needs in the region (Wei et al., 2004). Animal waste, i.e., yak dung, is the predominant energy source in the pastoral and agro-pastoral regions of the central Tibetan Plateau, including Lhasa (Wang, 2009; Chen et al., 2015). Two of the five prefecture-level cities in central Tibet, including Lhasa, display similar energy consumption structures, and the energy consumption structures of the other three cities in eastern and southeastern Tibet, including Nyingchi, are similar.

At each site, a mini-volume portable sampler (Airmetrics, Eugene, OR, USA) was used to collect the suspended particles and to deposit them onto 47-mm polycarbonate filters (Nuclepore, Whatman International Ltd., Maidstone, UK) with 0.2-μm pores. The operating flow rate of the sampler was 5 L min^{-1}. At the four urban sites, sampling activities were carried out on the roofs of hotels (approximately 5–15 m above ground level) for 3 h each. These sampling sites were surrounded by residences and roads. At the glacier site, the sampler was placed 1.5 m above the ground, and the sampling time was 5 h. After sampling, the filters were sealed in plastic cassettes and stored in a refrigerator at 4 °C until analysis. Air temperature and relative humidity were

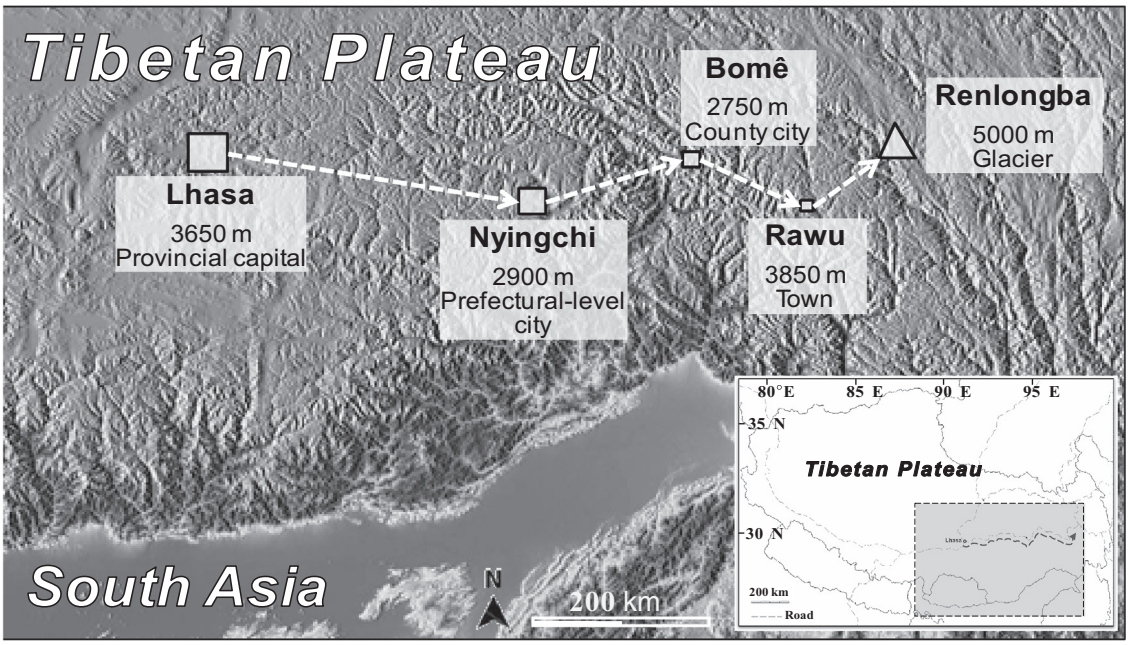

Fig. 1. Illustration of the sampling sites along the expedition route within the southeastern portion of the Tibetan Plateau. The elevation and administrative level of each site are shown in the boxes.

recorded by a portable Q-Trak Plus IAQ monitor (Model 7565, TSI Inc., Shoreview, MN, USA).

2.2. Sample analysis

Small rectangular sections (approximately 10 × 10 mm) were cut from the filters. The cut sections were fixed on stubs and coated with gold under vacuum. A scanning electron microscope (JEOL JSM-6460) was used to investigate and photograph the particles (Hu et al., 2009, 2011). The operating voltage was 20 kV. For each sample, 10 secondary electron images (SEI) were acquired with magnifications of 1000–30,000, depending on the sizes of the particles shown in the individual images.

The diameter of each individual particle was calculated as the average of the longest dimension and its orthogonal width; these dimensions were determined from the SEI images using IMAGE PRO PLUS (IPP) 5.0 software (Media Cybernetics, Inc., Silver Spring, MD, USA) (Hu et al., 2009, 2011). The aspect ratio (length/width) of a particle is defined as the ratio of its longest dimension to its orthogonal width, and this quantity was used to examine the compactness of the particles. Since it is difficult to estimate the losses of particles through the pores of the filters during sample collection, the particles smaller than 0.2 μm in each image were excluded from the size examination. In addition, scanning electron microscopes are not good at identifying organic particles, which usually causes an underestimate of organic particles.

The elemental compositions of the individual particles in each sample were analysed using a NORAN SYSTEM SIX Si-Li EDX detector with an ultra-thin window (Thermo Electron Corporation, Waltham, MA, USA), which was attached to the electron microscope (Hu et al., 2009, 2011). The EDX counting time for one particle was 30 s live time. To obtain statistical results, at least 300 particles were measured in each sample. X-ray peak intensities for each element were converted into weight fractions using the EDX software, which performs atomic number, absorption and fluorescence (ZAF) corrections.

In this study, backward air mass trajectories were applied to examine the possible source regions and transport pathways of aerosols at the Renlongba Glacier site. Three-day backward trajectories that began 500 m above the surface of the glacier during the sampling period (from 3:00 to 8:00 UTC on 18 April 2010) were calculated using the TrajStat software package (Wang et al., 2009), which is based on the HYSPLIT4 model developed by NOAA. The Global Data Assimilation System (GDAS) meteorological archive from NOAA was used to generate the trajectories. Wind fields at 500 hPa during the sampling period were from https://www.esrl.noaa.gov/psd/. Data from the European Centre for Medium-Range Weather Forecasts (ECMWF) showed that the planetary boundary layer height at the glacier site was 320–360 m when the samples were collected.

3. Results and discussion

3.1. Particle categories and number fractions

According to their morphologies and elemental compositions, the particles were categorized into six groups: soot aggregates, tar balls, soil dust particles, S-containing particles, coal fly ash, and biogenic particles (Fig. 2). The percentages of some types of particles might have been somewhat overestimated because of the low efficiency of the electron microscope in detecting small organic particles.

Both soot aggregates and tar balls contain large amounts of carbon (C), and these particles were identified based on their morphologies. Soot aggregates were the most frequently observed particle type, and they were distinguished from the other types by their distinctive chain-like or cluster-like morphologies. Each of the aggregates was composed of tens to hundreds of spherules, which were approximately 20 to 100 nm in size. Most of the soot aggregates were smaller than 0.5 μm in size. In these particles, C dominated, and the contents of oxygen (O) were small. Such particles frequently result from fossil fuel combustion and biomass burning (Novakov et al., 1997). Wildfires rarely occur on the elevated areas of the plateau, and no wildfires were reported during the expedition. Therefore, the soot particles we observed were produced by anthropogenic burning activities.

The tar balls were spherical particles that were usually smaller than 1 μm and were rarely agglomerated with other types of particles. Their elemental compositions were characterized by abundant C and minor amounts of O; trace amounts of potassium (K), chlorine (Cl) and sulfur (S) were found in some (but not all) of these particles. Tar balls are usually produced by biomass burning and fossil fuel combustion, especially

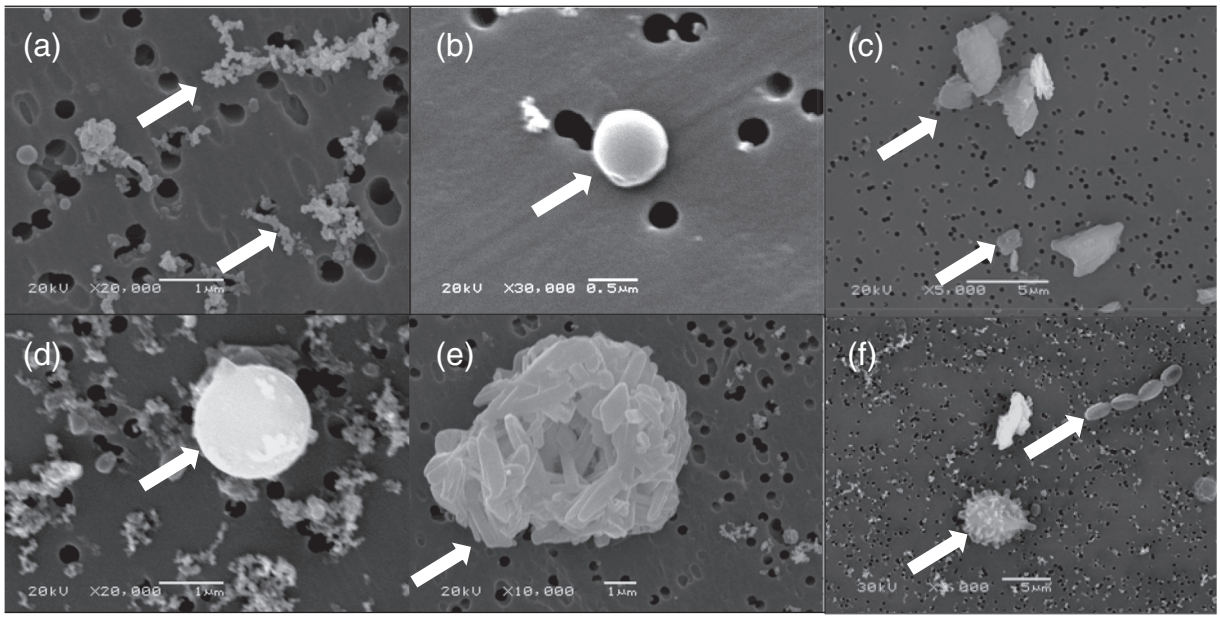

Fig. 2. Sample microscope images of particles from the six groups: (a) soot aggregates, (b) tar balls, (c) soil dust, (d) fly ash, (e) S-containing particles, and (f) biogenic particles.

through smouldering combustion (Li et al., 2003; Chakrabarty et al., 2006).

The identification of soil dust particles, fly ash, and S-containing particles was based on their predominantly inorganic elemental compositions; C, N and O were excluded to avoid interference from the filters (Okada and Kai, 2004). Sulfur-free particles with irregular shapes that were abundant in silicon (Si), aluminium (Al) and/or iron (Fe) were identified as soil dust particles, which are composed of aluminosilicates, silicates or Fe oxides. Fly ash particles were generally micron-size spherulites, and their compositions were similar to those of the soil dust particles; they were enriched in Al and Si, and they either did or did not contain relatively minor amounts of sodium (Na), magnesium (Mg), calcium (Ca), magnesium (Mn) and Fe.

Particles with weight percentages of elemental S exceeding 5% were classified as S-containing particles. They frequently occurred as aggregates or particles adhering to other particles, including soil dust and fly ash particles. Similar to soot particles, S-containing particles are usually generated by the anthropogenic combustion of S-containing fuel or vegetation; the S in these particles generally occurs in sulfate compounds. In addition to the particles described above, some biogenic particles were identified. These particles included pollen and spores that displayed clearly regular surfaces or symmetrical shapes, and their EDX spectra reflected enrichment in elemental C.

Based on the numbers of particles observed, soot aggregates, tar balls and soil dust particles were the most frequently observed types. Together, these types made up approximately 90% or more of the particles. The relative number percentages of the major particle types indicate that anthropogenic aerosols were abundant in the sampled urban air (Fig. 3). Soot and tar balls represented 73%, 80%, 85%, and 66% of the particles collected in Lhasa, Nyingchi, Bomê, and Rawu, respectively. These carbonaceous aerosols, i.e., soot aggregates and tar balls, collected at the urban sites were produced by local fossil fuel combustion and

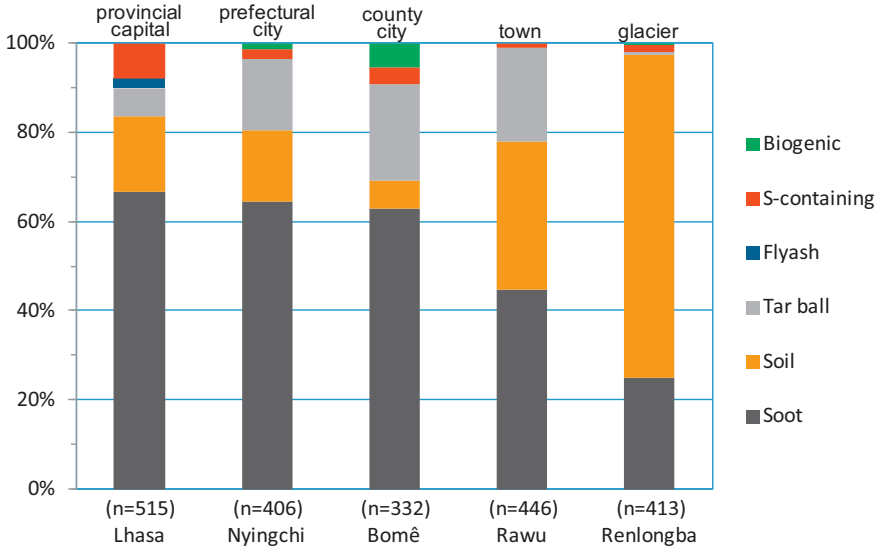

Fig. 3. Relative number percentages of the major particle types, ranked by urban area and population density. Values in parentheses indicate the numbers of particles analysed from the samples collected at each site.

biomass burning for heating, cooking and religious activities. Compared to the high abundance of carbonaceous particles, a small number of soil dust particles were noted in the urban samples. The number fractions of these particles were 6% at Bomê and 33% at Rawu. These particles were suspended in the roadside air by local circulation and traffic. Fly ash particles were observed only at Lhasa, where their abundance was 2%, reflecting their origin as a byproduct of coal combustion. Emissions from combustion of multiple fuels including biomass, coal and natural gas were also indicated by the high abundance of S-containing particles in the samples collected in Lhasa (8% by number); this abundance is one to six times greater than the corresponding values measured in the other cities. Biogenic particles were frequently detected in Nyingchi and Bomê, consistent with the flourishing forests near these two cities. The aerosols at the glacier site were characterized by soil dust particles (72%), followed by soot aggregates (25%), and a small number (approximately 3%) of tar balls, S-containing particles and biogenic particles.

The number fractions of major aerosol types were compared with the results of studies on aerosol particles at high-elevation sites using individual particle analysis methods (Table 1). The differences between the urban and remote aerosols were associated with the complexity of the aerosol particle types in the urban atmosphere and the high number fraction of soil dust particles at the remote glacier site. Among the main particle types, the frequently observed groups were soot aggregates, organic particles/tar balls, and soil/mineral dust, despite the variations in particle type identifications and the strategies used in the sampling and measurements. In previous studies, abundant soot particles were noted at Qomolangma (Cong et al., 2010), Nam Co (Cong et al., 2009; Hu et al., 2013), Shangri-La (Hu et al., 2013; Fan et al., 2016), and Menyuan (Li et al., 2015) and were attributed to long-range transport from regions outside of the plateau.

The abundance of tar balls varied dramatically with time and location. The abundance of tar balls was much lower at the glacier site than at the sites in the central region and on the eastern edge of the plateau. Tar balls derived from biomass smoke at other sites on the plateau were reported to fall within the size range of 200–600 nm (Cong et al., 2009, 2010). In this study, the large tar balls produced by the combustion of from firewood or other biofuels fell in the submicron size range at the urban sites, likely depending on sources and combustion conditions. Considering the pore size of the Nuclepore filters used in this study, the absence of fine tar balls might be caused by the poor collection efficiency of particles smaller than 0.2 μm. In the air of Lhasa, soot particles made up 67% of the particles collected. This result is consistent with those of previous studies conducted in Lhasa, which also report that soot particles are the most abundant type of anthropogenic particles (Zhang et al., 2001). The combustion of coal and biomass fuels and the vegetation burning as religious activities are still the major sources of anthropogenic particles in Lhasa. Soot aggregates (8%–30% by number) related to anthropogenic activities were frequently observed, including at the Renlongba glacier site. Compared to soil dust, soot particles have relatively low density; thus, their residence times in the atmosphere are long, and they can be transported over long distances from their source regions.

The number fractions of soil dust particles and soot aggregates were high at the remote glacier. The glacier site is located in a valley, and the valley breeze blew constantly during our sampling activities. The soil dust particles were likely derived from exposed surfaces in the surrounding areas. No sources of soot aggregates were present near the glacier site, suggesting that the aggregates were due to long-distance transport. The back-trajectory analysis indicated that the air masses arriving at Renlongba Glacier travelled through the eastern Himalayas and passed near Bomê and Nyingchi (Fig. 4). The wind field during our sampling period also indicates that the glacier area was under westerly winds and the air masses arriving at the glacier moved very slowly. Anthropogenic soot aggregates were abundant in the urban areas along the transport pathways. The abundance of soot (25%) in the glacier aerosols was lower than those in the cities (63%–67%) and the small town (45%). In the April when our expedition was conducted, westerly winds prevailed in the southeastern Tibetan Plateau and the glacier area was hardly influenced by air pollutants from South Asia. Therefore, the aerosol particles we collected were mainly from anthropogenic emissions at the surrounding areas within the plateau.

3.2. Particle size

The relative number fractions of the particles in different size ranges are shown in Fig. 5. The majority of particles fell within the submicron size range at both the urban (81%–97% by number) and glacier sites (70%). In this study, the percentage of submicron-sized particles at the glacier site was higher than those at Qomolangma (48%) (Cong et al., 2010) and Shangri-La (33%) (Fan et al., 2016) but lower than that at Nam Co (>90%) (Hu et al., 2013). Although the peaks of the particle size distributions at all of these sites fell between 0.2 and 0.3 μm, the

Table 1
Number percentages of individual major particle types at different remote (upper part) and urban (lower part) sites in the Himalayas and on the Tibetan Plateau.

Month/year	Site	Location	Altitude (m)	Soot	Tar balls	Soil dust	Fly ash	S-containing	Biogenic particles	Size (μm)	Reference
05-06/2005	Qomolangma	Central Himalayas	6520	8	3	60[a]	0	16	12	>0.4	Cong et al., 2010
07-08/2011	Shangri-La	Eastern margin of TP[b]	3580	19	c	52	29[c]	–	–	>0.8	Hu et al., 2013
07-08/2016	Shangri-La	Eastern margin of TP	3580	8	17[d]	36	6	31[d]	d	>0.2	Fan et al., 2016
09-10/2013	Menyuan	Northern margin of TP	3295	12[e]	–	5[e]	3[e]	–	–	>0.2	Li et al., 2015
03-05/2007	Nam Co	Central TP	4730	12	5	75[f]	0	7	1	>0.5	Cong et al., 2009
07-08/2011	Nam Co	Central TP	4730	30	26	44	0	–	–	>0.8	Hu et al., 2013
04/2010	Renlongba	Eastern Himalayas	5000	25	1	72	0	2	0	>0.2	This study
04/2010	Bomê	Eastern Himalayas	2750	63	22	6	0	4	5	>0.2	This study
04/2010	Nyingchi	Eastern Himalayas	2900	64	16	16	0	2	2	>0.2	This study
04/2010	Lhasa	Central TP	3650	67	6	17	2	8	0	>0.2	This study
08-10/1998,9	Lhasa	Central TP	3650	84	–	–	–	–	–	>0.3	Zhang et al., 2001
02/2013	Lhasa	Central TP	3667	10	–	90[g]	–	–	–	>0.8	Duo et al., 2015

[a] In this table, soil dust includes the aluminosilicate/silica, Ca/Mg carbonate, and Fe/Ti-rich particle types reported in this reference.
[b] "TP", Tibetan Plateau.
[c] Here, the tar ball and fly ash types are included in the "spherical particles" type (29% by number) reported in this reference.
[d] The tar ball and biogenic particle types are combined into the "organic particle" type, and the S-rich and K-rich types are incorporated into the "complex secondary particles" type (31% by number) reported in this reference.
[e] In this reference, the particle classification focuses on internal mixing states assessed using TEM, so the most abundant "secondary inorganic aerosol (SIA)" type (59% by number) and the "K-Na-Cl" type cannot be reported in this table. The data quoted here are based on particle number percentages measured at high pollution levels ($PM_{2.5} > 30\ \mu g\ m^{-3}$).
[f] The soil dust in this table combines the aluminosilicate/quartz, Ca/Mg carbonate, and Fe/Ti-rich particle types reported in this reference.
[g] The soil dust in this table combines the Si-rich, Ca-rich, Fe-rich, Al-rich, Pb-rich, K-rich, and other particle types, and it should be noted that the abundances of soot, tar balls, and fly ash were substantially underestimated in this reference; "-", no data are available.

Fig. 4. Three-day backward trajectories (500 m above the surface) of aerosols over the Renlongba Glacier site during the 5-hour sampling campaign.

relative values of the peaks differed between the sites. The peak was lowest at Lhasa (22%), due to the abundance of soil dust, fly ash, and S-containing particles in the city.

Compared to the provincial capital, the other three cities displayed higher peaks (49% in Bomê, 42% in Nyingchi, and 29% in Rawu), likely due to the use of firewood as an energy source. The peak number

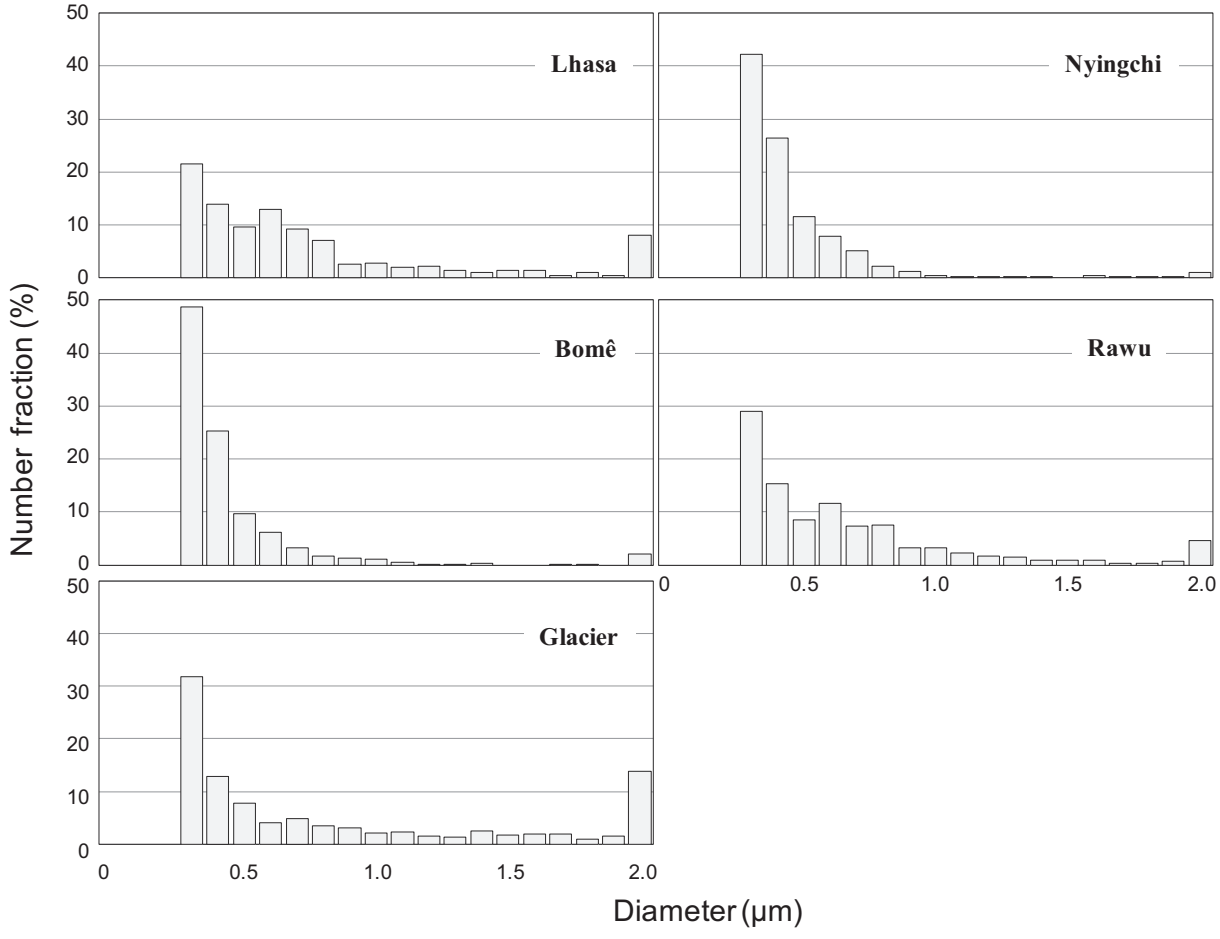

Fig. 5. Relative number fractions of particles by size at the urban sites and the glacier site. The size bin is 0.1 μm.

percentage at the glacier site was 32%. During atmospheric transport, particle size distributions may shift to smaller size ranges because gravitational settling preferentially removes large particles, rather than small particles (Mori et al., 2003).

The aerosols at the glacier site displayed a unimodal size distribution, similar to those at Bomê and Nyingchi, whereas the distributions noted at Lhasa and Rawu were bimodal and contained a lower second peak between 0.6 and 0.8 μm. The occurrence of the fine mode particles at the urban sites indicates that the cities are important regional sources of carbonaceous particles on the plateau. Also note that soot aggregates dominated the fine mode at sizes smaller than 0.5 μm at all of the urban sites. Given their small size, those particles would have long residence times in the atmosphere and could travel to remote areas, such as glaciers and ice caps. Similar fine mode soot particles from urban sources have frequently been observed at suburban and rural sites in several previous studies (Hasegawa and Ohta, 2002; Hudson et al., 2004; Mallet et al., 2004; Johnson et al., 2005; Adachi and Buseck, 2008; Moffet et al., 2010).

3.3. Transport of soot aggregates

To examine the transport of the soot aggregates, their number fractions according to size at the urban sites and the remote glacier site were compared (Fig. 6). The mode of the size distribution at the glacier site was similar to those at the urban sites. One small difference is that, at the glacier site, more of the particles fell in the small size range; approximately 87% of the particles were smaller than 0.5 μm. The corresponding percentages at Nyingchi and Bomê were 80% and 76%, respectively, slightly smaller than that at the glacier site. However, the corresponding percentages at Lhasa and Rawu were approximately 49%, much lower than that at the glacier site. Note that most of the soot particles fell in the submicron size range. Even at Lhasa and Rawu, where soot clusters were present, the percentages of soot aggregates in the size range larger than 1 μm were <9%. Soot particles larger than 2 μm were rarely observed.

The aspect ratios of the particles were calculated based on their sizes measured in the electron microscope images in order to investigate the changes in the shapes of the particles during transport. The aspect ratio of a particle, which is defined as the ratio of its longest dimension to its orthogonal width, is an indicator of particle compactness. Large aspect ratios indicate highly elongated particles (Okada et al., 2001; Adachi et al., 2010; Niu et al., 2012). The mean and standard deviations of the aspect ratios of the soot particles and all of the particles at each site are listed in Table 2. The aspect ratios of more than half of the soot particles (e.g., 52% in Lhasa, 68% in Bomê, and 64% on the glacier) were between 1.5–3.0 at all of the sites, indicating that the soot particles were not highly compact. Furthermore, both the highest soot peak size abundance (Fig. 6) and the largest aspect ratio (Table 2) occurred at the glacier site, indicating that small soot particles with low densities can easily be transported to glaciers and retain their chain-like structures.

Soot particles may undergo various ageing processes, such as coagulation, condensation and heterogeneous reactions, while travelling in the air. The ageing processes results in two types of changes in the particles. One of these types of changes affects the shapes of the particles, whereas the other involves the occurrence of salts, such as sulfates, in the particles (Pósfai et al., 2003; Johnson et al., 2005; Adachi and Buseck, 2008; Moffet et al., 2010). Shapes and mixing states may change significantly within several hours within urban environments, given the

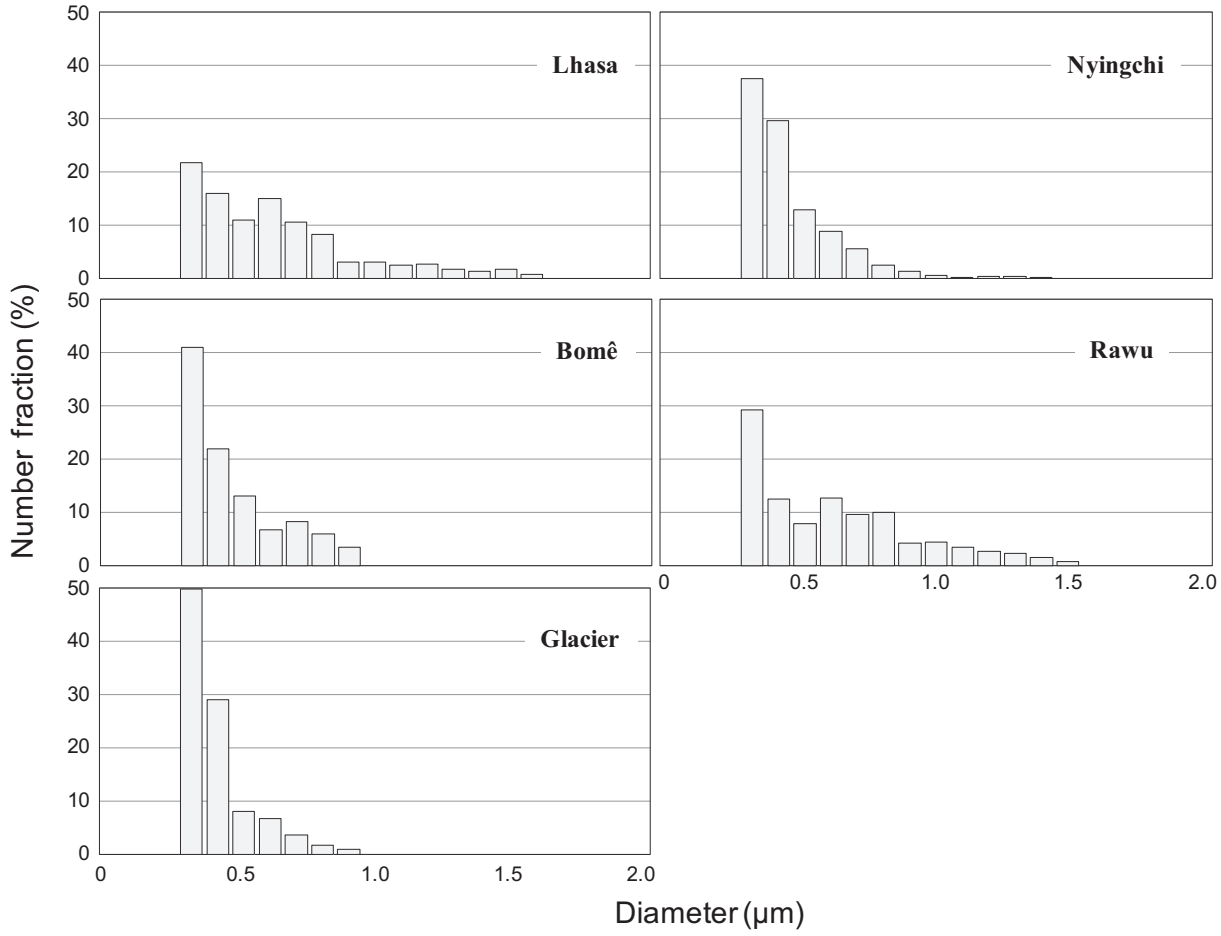

Fig. 6. Relative number fractions of soot aggregate particles by size at the urban sites and the glacier site.

Table 2
Mean aspect ratios and the standard deviations of the measured aspect ratios.

Aspect ratio	Lhasa	Nyingchi	Bomê	Rawu	Glacier
All particle types	1.6 ± 0.5	1.6 ± 0.5	1.8 ± 0.8	1.7 ± 0.7	1.7 ± 0.6
Soot	1.5 ± 0.3	1.6 ± 0.4	1.8 ± 0.7	1.7 ± 0.6	1.8 ± 0.6

presence of other aerosol particles (Johnson et al., 2005; Niu et al., 2011). In remote areas, long aerosol residence times result in more extensive processing, leading to more internally mixed soot/sulfate particles (Hasegawa and Ohta, 2002; Mallet et al., 2004; Niu et al., 2012).

However, the aspect ratios of the freshly emitted soot particles at the urban sites were not obviously different from those transported to the remote glacier in this study. Moreover, sulfur was detected in only a very few soot particles at the glacier site (<1% by number), and this percentage was lower than that noted in Lhasa, Nyingchi and Bomê. This result reflects weak chemical ageing of the particles during their movement to the glacier site. The occurrence of sulfate on particles is mainly influenced by the abundance of gas-phase SO_2 and/or the oxidizing capacity of the atmosphere (Pósfai et al., 2003). In a case involving stratospheric measurements in a biomass burning plume, with little SO_2 present and weak mixing with particles outside the plume, no sulfate was observed on biomass burning particles after long-range transport (Hudson et al., 2004). Primary particles experience very little chemical ageing when travelling in dry, cold air at high elevations, as noted in a previous study (Wu et al., 2012). The Tibetan Plateau is characterized by high altitudes, limited anthropogenic pollution and relatively low ozone column amounts (Ren et al., 1997; Dahlback et al., 2007). The emissions of sulfur dioxide due to anthropogenic activities there have been the smallest in China since official records began in 2003. Even in Lhasa, which has the largest urban population of any city on the plateau, the annual mean concentrations of SO_2 and PM_{10} in 2010 were only 7 μg m^{-3} and 48 μg m^{-3}, respectively. Furthermore, the relative humidity of the plateau air is low. Meteorological records show that the relative humidity during the period in which we collected our observations was 34% at Lhasa, 60% at Nyingchi, 68% at Bomê, 38% at Rawu, and 36% at the glacier site. Although the influx of solar radiation is expected to be strong on the plateau, the lack of precursor gases, oxidants and water vapor do not favour the chemical ageing of particles in the air. This slow chemical ageing of particles in the air likely accounts for the abundance of fresh soot particles at the glacier site.

Measurements made in the central Himalayas (Cong et al., 2010) and on the eastern edge of the Tibetan Plateau (Fan et al., 2016) have shown considerable percentages of fine S-containing soot particles. Those aged soot particles were attributed to long-range transport from South Asia and Southeast Asia, including pollutants from northern India (Cong et al., 2010) and northeastern Burma (Fan et al., 2016). Therefore, the physical and chemical properties of soot particles emitted and transported from cities and their surroundings on the Tibetan Plateau likely differ strongly from those emitted in areas outside the plateau.

A recent concern is the influence of soot (black carbon) particles on the albedos of glaciers and glacier retreat on the Tibetan Plateau. When deposited on glaciers, soot particles may darken glacier surfaces, increasing the absorption of sunlight and lengthening the melt season (Hansen and Nazarenko, 2004; B. Xu et al., 2009; B.Q. Xu et al., 2009). The mixing of soot aerosols with sulfate, nitrate and organic components during ageing usually magnifies their solar radiative forcing effects, causing climate warming, accelerating the melting of ice and snow (Jacobson, 2001; Schnaiter et al., 2005; Khalizov et al., 2009; Adachi et al., 2010) and changing the lifetimes of soot particles in the atmosphere (Ducret and Cachier, 1992; Sellegri et al., 2003). The fraction of soot particles mixed with sulfate, nitrate and organic components during ageing processes usually increases in both size and number, determining the magnitude of the solar radiation forcing (W. Li et al., 2016a, b). The soot particles we observed at the glacier were still fresh, in strong contrast to those transported to the Tibetan Plateau from South Asia. These particles were chain-like in shape, they were typically smaller than 0.5 μm in size, and they rarely contained secondary species such as sulfates. To our knowledge, these are the first observations showing that soot particles can remain in a fresh state with weak ageing while travelling in the atmosphere over Tibet. We cannot provide a quantitative assessment of the importance of this phenomenon at this stage because of the limited data that are available. However, quantifying the ageing process of soot particles that originate on the Tibetan Plateau is worthy of in-depth study because of the predominance of these particles in the plateau atmosphere and the possibly large difference in ageing state compared to particles from outside of the plateau.

4. Conclusion

In this study, we used a SEM to analyse aerosol particles collected at four urban sites and one remote glacier site in the southeastern portion of the Tibetan Plateau during an expedition conducted in spring 2010. The particles in the urban air samples were mainly soot aggregates, tar balls and S-containing particles that were likely produced mainly by human activities. At the glacier site, anthropogenic soot aggregates were frequently detected, in addition to mineral particles from nearby exposed surfaces. The modal size of the soot aggregates was similar to those of freshly emitted particles collected in the urban areas. The aspect ratios of the soot aggregates at the glacier site were close to those at the urban sites. Sulfur was detected in only a few (<1% by number) of these particles, indicating limited chemical ageing during transport that can be attributed to the lack of precursor gases and the low humidity of the air over the high-elevation plateau. These results indicate that the particles did not experience apparent physical or chemical ageing during their travel to the glacier site, which contrasts strongly with previous reports of soot particles transported from South Asia and found on the plateau. Backward trajectory analysis revealed that the air parcels that transported the soot aggregates to the glacier site moved very slowly before arriving at the site, indicating that the particles very likely originated on the plateau. The ageing process of soot particles in the air over the high-elevation plateau is likely to be very slow, in contrast to other areas. This distinctive phenomenon should receive additional attention in studies of the dispersion of anthropogenic soot particles and their subsequent effects in the atmosphere over Tibet.

Acknowledgements

This research is supported by the National Natural Science Foundation of China (41230641). Data analysis was partly supported by the JSPS KAKENHI Grant (JP16H02942).

References

Adachi, K., Buseck, P.R., 2008. Internally mixed soot, sulfates, and organic matter in aerosol particles from Mexico City. Atmos. Chem. Phys. 8 (21), 6469–6481.
Adachi, K., Chung, S.H., Buseck, P.R., 2010. Shapes of soot aerosol particles and implications for their effects on climate. J. Geophys. Res.-Atmos. 115 (D15).
Akimoto, H., 2003. Global air quality and pollution. Science 302 (5651), 1716–1719.
Bonasoni, P., Laj, P., Marinoni, A., Sprenger, M., Angelini, F., Arduini, J., Bonafè, U., Calzolari, F., Colombo, T., Decesari, S., Di Biagio, C., di Sarra, A.G., Evangelisti, F., Duchi, R., Facchini, M.C., Fuzzi, S., Gobbi, G.P., Maione, M., Panday, A., Roccato, F., Sellegri, K., Venzac, H., Verza, G.P., Villani, P., Vuillermoz, E., Cristofanelli, P., 2010. Atmospheric brown clouds in the Himalayas: first two years of continuous observations at the Nepal Climate Observatory-Pyramid (5079 m). Atmos. Chem. Phys. 10 (15), 7515–7531.
Buseck, P.R., Pósfai, M., 1999. Airborne minerals and related aerosol particles: effects on climate and the environment. Proc. Natl. Acad. Sci. 96 (7), 3372–3379.
Cao, J., Tie, X., Xu, B., Zhao, Z., Zhu, C., Li, G., Liu, S., 2010. Measuring and modeling black carbon (BC) contamination in the SE Tibetan Plateau. J. Atmos. Chem. 67 (1), 45.
Chakrabarty, R.K., Moosmüller, H., Garro, M.A., Arnott, W.P., Walker, J., Susott, R.A., Babbitt, R.E., Wold, C.E., Lincoln, E.N., Hao, W.M., 2006. Emissions from the laboratory combustion of wildland fuels: particle morphology and size. J. Geophys. Res.-Atmos. 111 (D7).

Chen, P., Kang, S., Bai, J., Sillanpää, M., Li, C., 2015. Yak dung combustion aerosols in the Tibetan Plateau: chemical characteristics and influence on the local atmospheric environment. Atmos. Res. 156, 58–66.
Cong, Z., Kang, S., Dong, S., Zhang, Y., 2009. Individual particle analysis of atmospheric aerosols at Nam Co, Tibetan Plateau. Aerosol Air Qual. Res. 9 (3), 323–331.
Cong, Z., Kang, S., Dong, S., Liu, X., Qin, D., 2010. Elemental and individual particle analysis of atmospheric aerosols from high Himalayas. Environ. Monit. Assess. 160 (1), 323–335.
Cong, Z., Kawamura, K., Kang, S., Fu, P., 2015. Penetration of biomass-burning emissions from South Asia through the Himalayas: new insights from atmospheric organic acids. Sci. Rep. 5, 9580.
Dahlback, A., Gelsor, N., Stamnes, J.J., Gjessing, Y., 2007. UV measurements in the 3000–5000 m altitude region in Tibet. J. Geophys. Res.-Atmos. 112, D09308.
Ducret, J., Cachier, H., 1992. Particulate carbon content in rain at various temperate and tropical locations. J. Atmos. Chem. 15 (1), 55–67.
Duo, B., Zhang, Y., Kong, L., Fu, H., Hu, Y., Chen, J., Li, L., Qiong, A., 2015. Individual particle analysis of aerosols collected at Lhasa City in the Tibetan Plateau. J. Environ. Sci. 29, 165–177.
Engling, G., Zhang, Y.N., Chan, C.Y., Sang, X.F., Lin, M., Ho, K.F., Li, Y.S., Lin, C.Y., Lee, J.J., 2011. Characterization and sources of aerosol particles over the southeastern Tibetan Plateau during the Southeast Asia biomass-burning season. Tellus Ser. B Chem. Phys. Meteorol. 63 (1), 117–128.
Fan, J., Shao, L., Hu, Y., Wang, J., Wang, J., Ma, J., 2016. Classification and chemical compositions of individual particles at an eastern marginal site of Tibetan Plateau. Atmos. Pollut. Res. 7 (5), 833–842.
Gao, J., Zhang, A., Lam, S.K., Zhang, X., Thomson, A.M., Lin, E., Jiang, K., Clarke, L.E., Edmonds, J.A., Kyle, P., Yu, S., Zhou, Y., Zhou, S., 2016. An integrated assessment of the potential of agricultural and forestry residues for energy production in China. GCB Bioenergy 8 (5), 880–893.
Hansen, J., Nazarenko, L., 2004. Soot climate forcing via snow and ice albedos. Proc. Natl. Acad. Sci. 101, 423–428.
Hasegawa, S., Ohta, S., 2002. Some measurements of the mixing state of soot-containing particles at urban and non-urban sites. Atmos. Environ. 36, 3899–3908.
Hu, T., Lee, S., Cao, J., Chow, J.C., Watson, J.G., Ho, K., Ho, W., Rong, B., An, Z., 2009. Characterization of winter airborne particles at Emperor Qin's Terra-cotta Museum, China. Sci. Total Environ. 407, 5319–5327.
Hu, T., Cao, J., Ho, K., An, Z., Lee, S., Chow, J.C., Watson, J.G., Li, H., 2011. Winter and summer characteristics of airborne particles inside Emperor Qin's Terra-Cotta Museum, China: a study by scanning electron microscopy-energy dispersive X-ray spectrometry. J. Air Waste Manage. Assoc. 61 (9), 914–922.
Hu, Y., Shao, L., Wang, J., Fan, J., Hou, C., 2013. Types and size distribution of individual particles in the Tibetan Plateau. Acta Petrol. Mineral. 32 (6), 863–872 (in Chinese with English abstract).
Hudson, P.K., Murphy, D.M., Cziczo, D.J., Thomson, D.S., De Gouw, J.A., Warneke, C., Holloway, J., Jost, H.J., Hübler, G., 2004. Biomass-burning particle measurements: characteristic composition and chemical processing. J. Geophys. Res.-Atmos. 109 (D23).
Jacobson, M.Z., 2001. Strong radiative heating due to the mixing state of black carbon in atmospheric aerosols. Nature 409, 695–697.
Johnson, K.S., Zuberi, B., Molina, L.T., Molina, M.J., Iedema, M.J., Cowin, J.P., Gaspar, D.J., Wang, C., Laskin, A., 2005. Processing of soot in an urban environment: case study from the Mexico City metropolitan area. Atmos. Chem. Phys. 5 (11), 3033–3043.
Kang, S., Xu, Y., You, Q., Flügel, W.A., Pepin, N., Yao, T., 2010. Review of climate and cryospheric change in the Tibetan Plateau. Environ. Res. Lett. 5 (1), 015101.
Kang, S., Chen, P., Li, C., Liu, B., Cong, Z., 2016. Atmospheric aerosol elements over the inland Tibetan Plateau: concentration, seasonality, and transport. Aerosol Air Qual. Res. 16, 789–800.
Kaufman, Y.J., Tanré, D., Boucher, O., 2002. A satellite view of aerosols in the climate system. Nature 419, 215–223.
Khalizov, A.F., Xue, H., Wang, L., Zheng, J., Zhang, R., 2009. Enhanced light absorption and scattering by carbon soot aerosol internally mixed with sulfuric acid. J. Phys. Chem. A 113 (6), 1066–1074.
Kopacz, M., Mauzerall, D.L., Wang, J., Leibensperger, E.M., Henze, D.K., Singh, K., 2011. Origin and radiative forcing of black carbon transported to the Himalayas and Tibetan Plateau. Atmos. Chem. Phys. 11 (6), 2837–2852.
Lau, K.M., Kim, M.K., Kim, K.M., 2006. Asian summer monsoon anomalies induced by aerosol direct forcing: the role of the Tibetan Plateau. Clim. Dyn. 26 (7–8), 855–864.
Lau, W.K., Kim, M.K., Kim, K.M., Lee, W.S., 2010. Enhanced surface warming and accelerated snow melt in the Himalayas and Tibetan Plateau induced by absorbing aerosols. Environ. Res. Lett. 5 (2), 025204.
Li, J., Pósfai, M., Hobbs, P.V., Buseck, P.R., 2003. Individual aerosol particles from biomass burning in southern Africa: 2, Compositions and aging of inorganic particles. J. Geophys. Res.-Atmos. 108 (D13), 8484.
Li, J., Lin, T., Qi, S., Zhang, G., Liu, X., Li, K., 2008. Evidence of local emission of organochlorine pesticides in the Tibetan plateau. Atmos. Environ. 42 (32), 7397–7404.
Li, W.J., Chen, S.R., Xu, Y.S., Guo, X.C., Sun, Y.L., Yang, X.Y., Wang, Z.F., Zhao, X.D., Chen, J.M., Wang, W.X., 2015. Mixing state and sources of submicron regional background aerosols in the northern Qinghai–Tibet Plateau and the influence of biomass burning. Atmos. Chem. Phys. 15 (23), 13365–13376.
Li, C., Bosch, C., Kang, S., Andersson, A., Chen, P., Zhang, Q., Cong, Z., Chen, B., Qin, D., Gustafsson, Ö., 2016. Sources of black carbon to the Himalayan–Tibetan Plateau glaciers. Nat. Commun. 7, 12574.
Li, Y., Chen, J., Kang, S., Li, C., Qu, B., Tripathee, L., Yan, F., Zhang, Y., Guo, J., Gul, C., Qin, X., 2016. Impacts of black carbon and mineral dust on radiative forcing and glacier melting during summer in the Qilian Mountains, northeastern Tibetan Plateau. Cryosphere 1–14.
Li, W., Shao, L., Zhang, D., Ro, C.-U., Hu, M., Bi, X., Geng, H., Matsuki, A., Niu, H., Chen, J., 2016a. A review of single aerosol particle studies in the atmosphere of East Asia: morphology, mixing state, source, and heterogeneous reactions. J. Clean. Prod. 112, 1330–1349.
Li, W., Sun, J., Xu, L., Shi, Z., Riemer, N., Sun, Y., Fu, P., Zhang, J., Lin, Y., Wang, X., Shao, L., Chen, J., Zhang, X., Wang, Z., Wang, W., 2016b. A conceptual framework for mixing structures in individual aerosol particles. J. Geophys. Res.-Atmos. 121 (22), 13784–13798.
Li, H., He, Q., Song, Q., Chen, L., Song, Y., Wang, Y., Lin, K., Xu, Z., Shao, M., 2017. Diagnosing Tibetan pollutant sources via volatile organic compound observations. Atmos. Environ. 166, 244–254.
Li, X., Kang, S., He, X., Qu, B., Tripathee, L., Jing, Z., Paudyal, R., Li, Y., Zhang, Y., Yan, F., Li, G., Li, C., 2017. Light-absorbing impurities accelerate glacier melt in the Central Tibetan Plateau. Sci. Total Environ. 587, 482–490.
Liu, G., Shen, L., 2007. Quantitive appraisal of biomass energy and its geographical distribution in China. J. Nat. Resour. 22 (1), 9–19 (in Chinese with English abstract).
Liu, X., Yin, Z.Y., 2002. Sensitivity of East Asian monsoon climate to the uplift of the Tibetan Plateau. Palaeogeogr. Palaeoecol. 183 (3), 223–245.
Loewen, M., Kang, S., Armstrong, D., Zhang, Q., Tomy, G., Wang, F., 2007. Atmospheric transport of mercury to the Tibetan Plateau. Environ. Sci. Technol. 41 (22), 7632–7638.
Lu, Z., Streets, D.G., Zhang, Q., Wang, S., 2012. A novel back-trajectory analysis of the origin of black carbon transported to the Himalayas and Tibetan Plateau during 1996–2010. Geophys. Res. Lett. 39, L01809.
Lüthi, Z.L., Škerlak, B., Kim, S.W., Lauer, A., Mues, A., Rupakheti, M., Kang, S., 2015. Atmospheric brown clouds reach the Tibetan Plateau by crossing the Himalayas. Atmos. Chem. Phys. 15 (11), 6007–6021.
Mallet, M., Roger, J.C., Despiau, S., Putaud, J.P., Dubovik, O., 2004. A study of the mixing state of black carbon in urban zone. J. Geophys. Res.-Atmos. 109, D04202.
Moffet, R.C., Henn, T.R., Tivanski, A.V., Hopkins, R.J., Desyaterik, Y., Kilcoyne, A.L.D., Tyliszczak, T., Fast, J., Barnard, J., Shutthanandan, V., Cliff, S.S., Perry, K.D., Laskin, A., Gilles, M.K., 2010. Microscopic characterization of carbonaceous aerosol particle aging in the outflow from Mexico City. Atmos. Chem. Phys. 10 (3), 961–976.
Mori, I., Nishikawa, M., Tanimura, T., Quan, H., 2003. Change in size distribution and chemical composition of kosa (Asian dust) aerosol during long-range transport. Atmos. Environ. 37 (30), 4253–4263.
Niu, H., Shao, L., Zhang, D., 2011. Aged status of soot particles during the passage of a weak cyclone in Beijing. Atmos. Environ. 45 (16), 2699–2703.
Niu, H., Shao, L., Zhang, D., 2012. Soot particles at an elevated site in eastern China during the passage of a strong cyclone. Sci. Total Environ. 430, 217–222.
Novakov, T., Cachier, H., Clark, J.S., Gaudichet, A., Macko, S., Masclet, P., 1997. Characterization of particulate products of biomass combustion. In: Clark, J.S., Cachier, H., Goldammer, J.G., Stocks, B. (Eds.), Sediment records of biomass burning and global change. NATO ASI Series (Series I: Global Environmental Change), vol. 51. Springer, Berlin, Heidelberg.
Okada, K., Kai, K., 2004. Atmospheric mineral particles collected at Qira in the Taklamakan Desert, China. Atmos. Environ. 38 (40), 6927–6935.
Okada, K., Heintzenberg, J., Kai, K., Qin, Y., 2001. Shape of atmospheric mineral particles collected in three Chinese arid-regions. Geophys. Res. Lett. 28 (16), 3123–3126.
Peng, J., Liu, Z., Liu, Y., Wu, J., Han, Y., 2012. Trend analysis of vegetation dynamics in Qinghai - Tibet Plateau using Hurst exponent. Ecol. Indic. 14 (1), 28–39.
Pósfai, M., Simonics, R., Li, J., Hobbs, P.V., Buseck, P.R., 2003. Individual aerosol particles from biomass burning in southern Africa: 1. Compositions and size distributions of carbonaceous particles. J. Geophys. Res.-Atmos. 108 (D13), 8483.
Ramanathan, V., Feng, Y., 2009. Air pollution, greenhouse gases and climate change: global and regional perspectives. Atmos. Environ. 43, 37–50.
Ren, P.B.C., Sigernes, F., Gjessing, Y., 1997. Ground-based measurements of solar ultraviolet radiation in Tibet: preliminary results. Geophys. Res. Lett. 24 (11), 1359–1362.
Schnaiter, M., Linke, C., Möhler, O., Naumann, K.H., Saathoff, H., Wagner, R., Schurath, U., 2005. Absorption amplification of black carbon internally mixed with secondary organic aerosol. J. Geophys. Res.-Atmos. 110, D19204.
Sellegri, K., Laj, P., Dupuy, R., Legrand, M., Preunkert, S., Putaud, J.P., 2003. Size-dependent scavenging efficiencies of multicomponent atmospheric aerosols in clouds. J. Geophys. Res.-Atmos. 108 (D11), 4334.
Wang, Q., 2009. Prevention of Tibetan eco-environmental degradation caused by traditional use of biomass. Renew. Sust. Energ. Rev. 13 (9), 2562–2570.
Wang, Y.Q., Zhang, X.Y., Draxler, R.R., 2009. TrajStat: GIS-based software that uses various trajectory statistical analysis methods to identify potential sources from long-term air pollution measurement data. Environ. Model. Softw. 24 (8), 938–939.
Wei, X., Yang, P., Wang, Y., Xie, Z., 2004. Use of rural energy resources and eco-environmental degradation in Tibet. J. Environ. Sci. 16 (6), 1046–1050.
Wu, F., Zhang, D., Cao, J., Xu, H., An, Z., 2012. Soil-derived sulfate in atmospheric dust particles at Taklimakan desert. Geophys. Res. Lett. 39 (24).
Xia, X., Zong, X., Cong, Z., Chen, H., Kang, S., Wang, P., 2011. Baseline continental aerosol over the central Tibetan plateau and a case study of aerosol transport from South Asia. Atmos. Environ. 45 (39), 7370–7378.
Xu, B., Cao, J., Hansen, J., Yao, T., Joswia, D.R., Wang, N., Wu, G., Wang, M., Zhao, H., Yang, W., Liu, X., He, J., 2009. Black soot and the survival of Tibetan glaciers. Proc. Natl. Acad. Sci. 106 (52), 22114–22118.
Xu, B.Q., Wang, M., Joswiak, D.R., Cao, J.J., Yao, T.D., Wu, G.J., Yang, W., Zhao, H.B., 2009. Deposition of anthropogenic aerosols in a southeastern Tibetan glacier. J. Geophys. Res.-Atmos. 114 (D17).
Yanai, M., Li, C., Song, Z., 1992. Seasonal heating of the Tibetan Plateau and its effects on the evolution of the Asian summer monsoon. J. Meteorol. Soc. Jpn. 70 (1B), 319–351.
Yang, Y.J., Renciluobu, Li, Cangla, J.X., 2008. Replacement of traditional domestic biofuels in Tibet. Sci. Technol. Tibet 184 (7), 32–35 (in Chinese without English abstract).

Yearbook, 2016. China Statistical Yearbook. National Bureau of statistics of China.
Zhang, D., Iwasaka, Y., Shi, G., 2001. Soot particles and their impacts on the mass cycle in the Tibetan atmosphere. Atmos. Environ. 35 (34), 5883–5894.
Zhang, N., Cao, J., Ho, K., He, Y., 2012. Chemical characterization of aerosol collected at Mt. Yulong in wintertime on the southeastern Tibetan Plateau. Atmos. Res. 107, 76–85.
Zhang, L., Guo, H., Ji, L., Lei, L., Wang, C., Yan, D., Li, B., Li, J., 2013. Vegetation greenness trend (2000 to 2009) and the climate controls in the Qinghai-Tibetan Plateau. J. Appl. Remote. Sens. 7 (1), 073572.
Zhang, X., Ming, J., Li, Z., Wang, F., Zhang, G., 2017. The online measured black carbon aerosol and source orientations in the Nam Co region, Tibet. Environ. Sci. Pollut. Res. 24 (32), 25021–25033.
Zhao, S., Ming, J., Sun, J., Xiao, C., 2013. Observation of carbonaceous aerosols during 2006–2009 in Nyainqêntanglha Mountains and the implications for glaciers. Environ. Sci. Pollut. Res. 20 (8), 5827–5838.
Zhao, Z., Cao, J., Shen, Z., Xu, B., Zhu, C., Chen, L.W.A., Su, X., Liu, S., Han, Y., Wang, G., Ho, K., 2013. Aerosol particles at a high-altitude site on the Southeast Tibetan Plateau, China: implications for pollution transport from South Asia. J. Geophys. Res.-Atmos. 118 (19), 11360–11375.
Zhu, J., Xia, X., Che, H., Wang, J., Zhang, J., Duan, Y., 2016. Study of aerosol optical properties at Kunming in sourthwest China and long-range transport of biomass burning aerosols from North Burma. Atmos. Res. 169, 237–247.
Zhu, J., Xia, X., Wang, J., Zhang, J., Wiedinmyer, C., Fisher, J.A., Keller, C., 2017. Impact of Southeast Asian smoke on aerosol properties in Southwest China: first comparison of model simulations with satellite and ground observation. J. Geophys. Res. 122. https://doi.org/10.1002/2016JD025793.